ELSEVIER

Nuclear Instruments and Methods in Physics Research A 462 (2001) 411–425

NUCLEAR INSTRUMENTS & METHODS IN PHYSICS RESEARCH Section A

www.elsevier.nl/locate/nima

Beam tests of a thin dual-readout calorimeter for detecting cosmic rays outside the Earth's atmosphere

Vladimir Nagaslaev, Alan Sill, Richard Wigmans*

Department of Physics, Texas Tech University, Box 41051, Lubbock, TX 79409-1051, USA

Received 13 April 2000; received in revised form 5 September 2000; accepted 17 October 2000

Abstract

Cosmic ray experiments outside the Earth's atmosphere are subject to very severe restrictions on the mass of the instruments. Therefore, it is important that the experimental information that can be obtained per unit detector mass is maximized. In this paper, we describe tests of a thin ($1.4\lambda_{\mathrm{int}}$ deep) hadron calorimeter that was designed with this goal in mind. This detector was equipped with two independent active media, which provided complementary information on the showering hadrons. It is shown that by combining the information from these media it was possible to reduce the effects of the dominant leakage fluctuations on the calorimeter performance.

PACS: 13.85.Tp; 29.40.Vj; 07.60.Vg

Keywords: Calorimetry; Optical fibers; Cosmic rays

1. Introduction

In recent years, there has been an increased interest in the use of calorimetric techniques in cosmic-ray experiments outside the Earth's atmosphere. Calorimeters have been applied in experiments carried out in stratospheric balloon flights, in satellites and in the Space Shuttle. Several experiments are currently being planned for the International Space Station (ISS). These experiments focus on measuring features of the cosmic rays that are inaccessible with Earth-bound detectors, e.g., the antiproton content, the chemical and isotopic composition and the high-energy electron and photon spectra.

One common aspect of all these experiments is the severe restriction on the mass of the detectors. It is extremely expensive to bring massive instruments into an orbit around the Earth. For calorimeters, this restriction poses a new challenge: *How to maximize the calorimetric information per unit detector mass*, or in other words: *How to minimize the detector mass, commensurate with experimental requirements* (energy resolution, detector acceptance, etc.)

The high-energy (> 1 GeV) cosmic-ray spectra are well described with a power-law: $\mathrm{d}N/\mathrm{d}E \sim E^{-3}$. A modest energy resolution ($\sim 30\%$) is considered good enough in most experiments. However, because of the steeply falling spectra,

*Corresponding author. Tel. +1-806-742-3779; fax: +1-806-742-1182.

E-mail address: wigmans@ttu.edu (R. Wigmans).

0168-9002/01/$ - see front matter
PII: S0168-9002(01)00185-1

the *shape of the response function* is extremely important. Tails in this function may completely and irrepairably distort the measured spectra.

When high-energy hadrons develop showers in a 1–2λ_{int} deep calorimeter, the response function is completely determined by leakage fluctuations. These fluctuations are very likely correlated with the fraction of energy spent on π^0 production inside the detector. In general, π^0s produced in the first nuclear interaction develop em showers that are contained in the detector, while charged pions typically escape. Therefore, events in which a large fraction of the initial energy is converted in π^0s in the first interaction will exhibit little leakage (a large detector signal), while events in which a small fraction of the energy has been transferred to π^0s will be characterized by large leakage (small detector signals).

It has been demonstrated experimentally that calorimeters using quartz fibers as active material are in practice almost exclusively sensitive to the π^0 component of hadron showers [1]. This is because Cherenkov light, which forms the source of experimental information in such calorimeters is emitted by shower particles down to energies below 1 MeV in the electromagnetic (em) showers initiated by π^0s, while in the non-em component of hadron showers, most of the energy is deposited by non-relativistic particles [2].

In the present study, we have used this feature in an attempt to get a handle on the (leakage) fluctuations that dominate the performance of very thin hadron calorimeters, and thus improve this performance. Since these fluctuations are presumably correlated to π^0 production in the first hadronic interaction in the calorimeter, as argued above, a measurement of the fraction of the total measured hadron signal that is caused by the em shower component would provide such a handle.

A dual-readout calorimeter that measures both the ionization losses ($\mathrm{d}E/\mathrm{d}x$) and the production of Cherenkov light, might thus distinguish between events with relatively small and large shower leakage, since the ratio of the two signals would be different in these two cases: A relatively large Cherenkov signal would indicate relatively little shower leakage, while a small Cherenkov signal (compared to the $\mathrm{d}E/\mathrm{d}x$ signal) would suggest that a large fraction of the shower energy escaped from the detector.

We have built and tested such a calorimeter, in the framework of prototype studies for the Advanced Cosmic Composition Experiment at the Space Station (ACCESS). In this paper, we describe results of beam tests of this calorimeter, which were primarily aimed to study to what extent the performance of a thin hadron calorimeter may be improved if the $\mathrm{d}E/\mathrm{d}x$ information is complemented with measurements of the production of Cherenkov light. In Section 2, the calorimeter and the setup in which it was tested are described in some detail. The experimental results of these tests are described, analyzed and discussed in Section 3. A summary and conclusions are given in Section 4.

2. Experimental setup

2.1. The calorimeter

The calorimeter used for the studies described in this paper consisted of 39 lead plates (with a thickness of 6.4 mm each, for a total depth of 1.4 λ_{int} or $46X_0$). These plates were interleaved with alternating ribbons of scintillating and quartz fibers, providing x,y-readout and an effective tower structure for particles entering perpendicular to the absorber plates, for both types of light (Fig. 1).

The scintillating fibers[1] were 500 μm thick (a 440 μm cylindrical core surrounded by a 30 μm thick cladding consisting of 15 μm PMMA and 15 μm fluorinated plastic) and had a numerical aperture of 0.72. The quartz fibers[2] were 270 μm thick (a 210 μm thick quartz core, surrounded by a 10 μm thick silicone cladding and a 20 μm nylon jacket) and their numerical aperture was 0.40. The showering particles generated scintillation light in the plastic fibers and Cherenkov light in the quartz fibers. Photons emitted within the numerical aperture of the fibers were captured and

[1] SCSN-81, a polystyrene-based product manufactured by Kuraray Inc., Japan.

[2] Manufactured by Fiberguide Industries, USA.

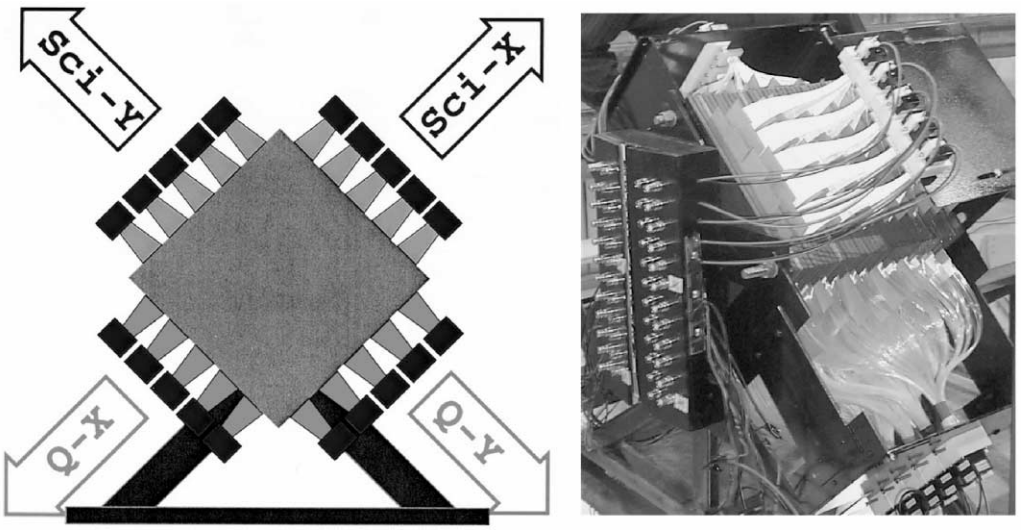

Fig. 1. Schematic layout and a photograph of the dual-readout calorimeter. Thin lead plates are interleaved with 4 cm wide ribbons of scintillating and quartz fibers, which both provide readout in two coordinates.

transported through internal reflection to the fiber ends, where they were converted into photoelectrons in the photocathode of a photomultiplier tube (PMT). The digitized output of these PMTs comprised the calorimeter signals.

The fiber ribbons were inserted between the absorber plates according to the following scheme (see also Fig. 3). Plate 1 was followed by a layer of quartz fibers oriented in the x direction (Q_x), plate 2 by a layer of quartz fibers oriented in the y direction (Q_y). The first layer of scintillating fibers (S_x, oriented in the x direction) was located behind absorber plate 3. Plates 4–6 were followed by layers of the types Q_x, Q_y and S_y, respectively. This pattern for the first six sampling layers was repeated subsequently. In total, the calorimeter contained 13 sampling layers of the types Q_x and Q_y each and six sampling layers of the types S_x and S_y each.

Each fiber layer consisted of five 40 mm wide ribbons. They were inserted in 1 mm wide slots between the absorber layers. The instrumented detector volume thus comprised a surface area of 20×20 cm^2 that extended over a depth of 28 cm. The length of the fibers varied between 40 and 55 cm. The five ribbons were read out separately, combined with the corresponding ribbons located at other depths in the structure. For example, the S_x ribbons located behind absorber layers #3, 9, 15, 21, 27 and 33 were ganged together into five bunches and read out by five PMTs. The Q_x ribbons behind absorber layers #1, 4, 7, 10, 13, 16, 19, 22, 25, 28, 31, 34 and 37 were ganged together in five bunches read out by five other PMTs. Also the S_y and Q_y ribbons were read out by five PMTs each, giving a total of 20 electronic channels.

Because of the way the signals from the active material were read out, the calorimeter had a tower structure for particles entering it perpendicular to its front surface (i.e., at a 90° angle with the fibers). In total, there were 25 square cylindrical towers, each with a cross-section of 4×4 cm^2, both for the scintillating-fiber and quartz-fiber signal readout.

The calorimeter contained in total $\sim 20\,000$ quartz fibers and ~ 4800 scintillating fibers. The fiber bunches were machined and polished and coupled with an air gap to a Hamamatsu metal-channel PMT.[3] During our tests, these PMTs were operated at a gain of typically a few times 10^5.

[3] R5900U, 10-stage.

Before the detector was assembled, all fiber ribbons and PMTs were individually tested with a radioactive source (^{106}Ru) and with a Light Emitting Diode. In these tests, the production of (scintillation) light in and the transmission of light through the fibers were measured, as well as the gain-voltage characteristics of all PMTs.

Fig. 2 shows an example of the results of these tests. In this figure, the response of the 12 individual scintillating-fiber ribbons to the β particles emitted by a ^{106}Ru source is plotted. The position of the source with respect to the ribbon and the PMT used to collect the light were the same in these tests. The ribbon-to-ribbon response fluctuations were found to be smaller than 5%.

The parameters relevant for the development of showers in this calorimeter had the following values. The radiation length was 0.65 cm, the Molière radius was 1.85 cm, and the nuclear interaction length for protons was 19.7 cm. The sampling fraction for minimum ionizing particles was 0.28% for the scintillating fibers ($S_x + S_y$) and 0.53% for the quartz fibers ($Q_x + Q_y$).

2.2. The beam line

The measurements described in this paper were performed in the H2 beam line of the Super Proton Synchrotron at CERN. The detectors were mounted on a platform that could be moved vertically and laterally with respect to the beam, so that the center of each tower could be moved into the beam, as needed for calibration purposes. For most of the measurements, the angle (θ) between the beam and the calorimeter's front face was 0°. However, we also performed some measurements in which the detector was rotated, over angles up to $\theta = 90°$.

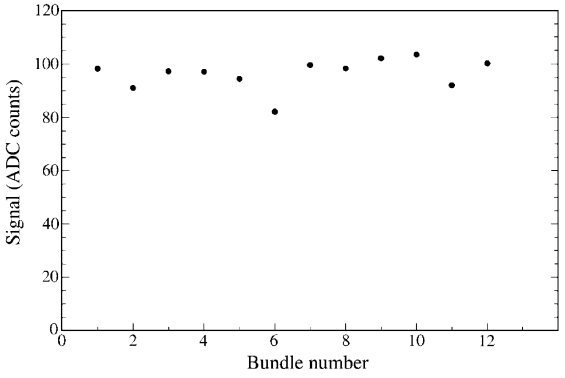

Fig. 2. The response of the 12 individual scintillating-fiber ribbons to the β particles emitted by a ^{106}Ru source.

Upstream of the calorimeter, a trigger counter telescope was installed. It consisted of 5 scintillation counters of different sizes (from 2×2 to 10×10 cm^2), which allowed a choice of the beam spot size for the recorded events. Downstream of the calorimeter, a large scintillation counter was installed (the "tail catcher"). Some of the measurements were carried out with a target installed directly in front of the calorimeter. This target consisted of two blocks of carbon, with a thickness of $0.25\lambda_{\text{int}}$ each. Three scintillation counters (Crb1–3, see Fig. 3) made it possible to select events in which the beam particle had interacted in the first or second of these two blocks, or in which the beam particles penetrated the target without undergoing a strong interaction.

Most of the hadron data analysis described in this paper was carried out with samples of events in which the particles interacted in the downstream carbon block. In these events, counters Crb1,2 produced signals compatible with that of a minimum ionizing particle (mip), while the signal from counter Crb3 was required to be larger than 3 mip. Typically, 15–20% of the events met these selection criteria. One might worry that the requirement of a relatively large signal in Crb3 could bias the event sample, and in particular lead to selecting events with an anomalously large em shower content. However, studies in which we varied the Crb3 threshold demonstrated that this was not the case. This may be understood from the fact that the radiation length of carbon is very long ($0.5\lambda_{\text{int}}$). Therefore, γs from the decay of π^0s produced in the interactions typically escaped from the target without contributing to the Crb3 signals, and converted in the lead absorber of the calorimeter.

In the electron measurements, the carbon target was replaced by a Preshower Detector, consisting of a 5 mm thick lead plate, followed by a

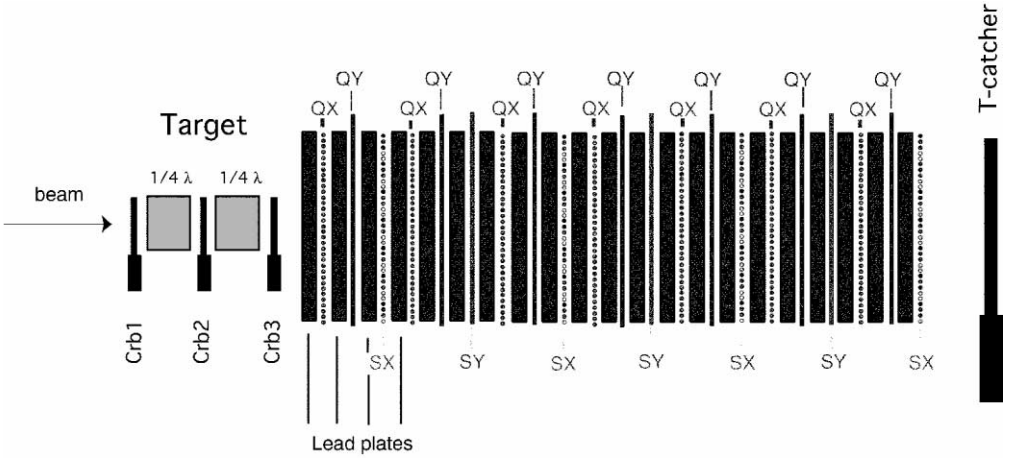

Fig. 3. Setup in the H2 beam line at CERN. Only 21 out of 39 calorimeter planes are shown. The calorimeter was preceded by a carbon target ($2 \times 0.25\lambda_{int}$ thick), instrumented with three scintillator planes. Downstream of the calorimeter, a tail catcher was installed.

scintillation counter. This device turned out to be very useful for eliminating hadron and muon contamination at very high energies. By requiring a signal larger than five times the minimum-ionizing value in the scintillation counter, events caused by the contaminating particles were almost completely eliminated, whereas almost all electrons passed this cut.

The hadron beam used for the tests described in this paper was a polarity and momentum selected secondary beam produced by 450 GeV protons incident on a target located about 550 m upstream of the calorimeter. We used this beam both in the positive and negative polarity mode, for energies ranging from 200 to 375 GeV. In this energy range, the negative beam consisted almost exclusively of π^- particles. The positive beam consisted of a mixture of protons and π^+, the proton fraction rapidly increasing with energy. This difference between the composition of the positive and negative beams was evident from the different event rates. At the highest energy used in these tests (375 GeV), near the kinematic limit, the event rates in the positive beam were more than an order of magnitude larger than in the negative beam.

We also used a tertiary beam for studies with electrons and low-energy pions. This beam was derived from a neutral secondary beam, which consisted predominantly of γs, K^0s and Λ^0s. Electrons and positrons were produced by putting a high-Z radiator in this beam.

During the tests described below, the beam particle rates varied between several hundred and several thousand events per spill. The spills lasted 2.6 s and were repeated every 14 s. The widths of the collimators in the beam line were chosen such that the contribution of the momentum uncertainty of the beam particles was negligible.

2.3. Readout and calibration

The calorimeter signals were transported through 80 m long RG-58 cables to the counting room. The signals were fed into Analog-to-Digital Converters (ADCs) with a dynamic range of 11 bits and a least count corresponding to 0.25 pC, which were operated at a gate width of 100 ns.

All individual cells of both calorimeters were calibrated with 150 GeV electrons incident on the cell center. The PMT gains were chosen in such a way that the average signal for 150 GeV electrons entering in the center of a cell corresponded to about 75 ADC counts above the pedestal value for the quartz fiber readout of that cell, and to 800 ADC counts for the scintillating fibers.

The stability of the calibration was checked several times during the test periods (typically every 2 days) by sending a 150 GeV electron beam

into the center of each and every calorimeter cell and measuring the signal distribution. The mean values of these distributions were reproduced to better than 5% in these measurements, for all channels.

3. Experimental results

3.1. Electrons

The detector was exposed to beams of electrons with energies of 50, 100, 150, 200, 250 and 300 GeV. Signal distributions recorded at 200 GeV are shown in Fig. 4.

Figs. 4a and b show the distributions measured with the scintillating fibers and the quartz fibers, respectively. The signals from the x and y fibers were added for this purpose. Both signal distributions are well described by a Gaussian function, as illustrated by the Gaussian curves, superimposed on the histograms, that were used to fit the experimental data. At this energy, the energy resolution measured with the scintillating fibers is 3.8%, vs. 10.0% for the quartz fibers.

Both resolutions were measured to scale with $E^{1/2}$. This is illustrated in Fig. 5, where the energy resolution, measured with both types of fibers, is plotted as a function of energy, on a scale that is linear in $E^{-1/2}$. In this plot, $E^{-1/2}$ scaling is thus described by a straight line through the bottom right corner of the graph (zero resolution at

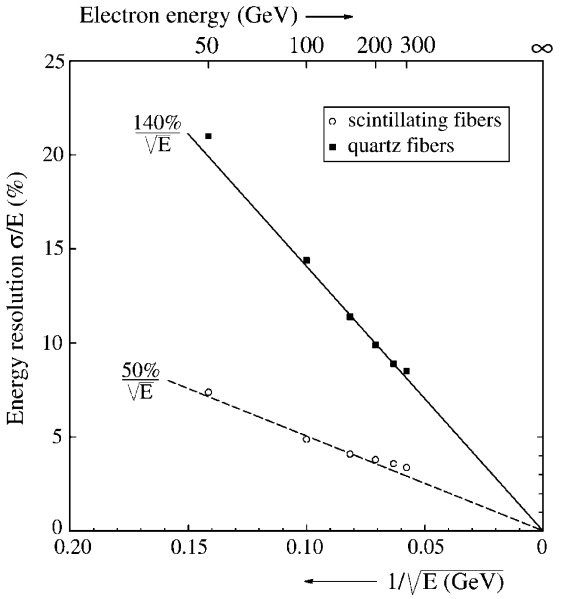

Fig. 5. The resolution for electrons, measured separately with the signals from the scintillating fibers and the quartz fibers, as a function of energy. The horizontal scale is linear in $E^{-1/2}$. The curves are drawn to guide the eye.

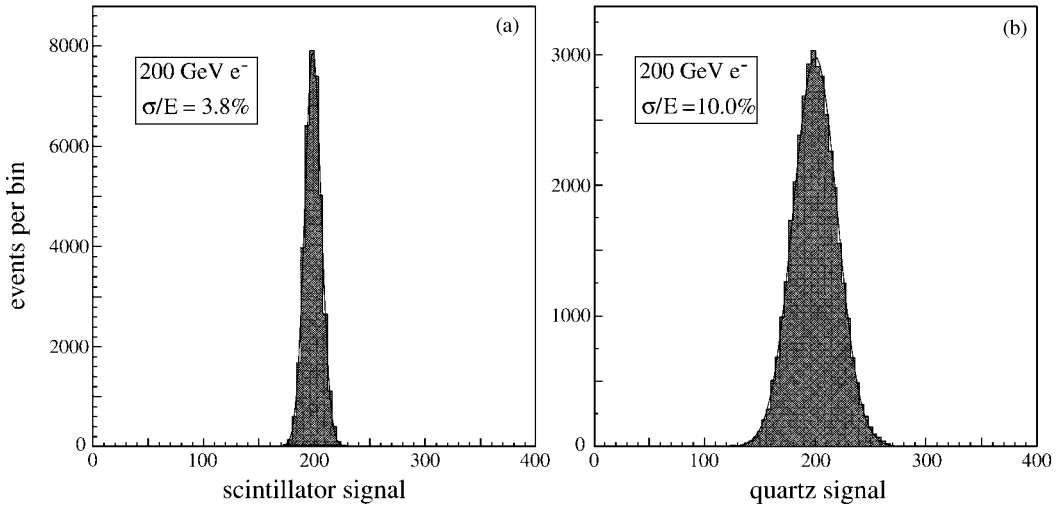

Fig. 4. Response function of the calorimeter for 200 GeV electrons. Shown are the signal distributions in the scintillating fibers (a) and in the quartz fibers (b).

infinite energy). These curves indicate that the energy resolution, σ/E, is well described by $50\%/\sqrt{E}$ for the scintillating fibers, and by $140\%/\sqrt{E}$ for the quartz fibers, with the energy E expressed in GeV.

Both the sampling fraction and the sampling frequency of the showers are higher for the quartz fibers than for the scintillating fibers. Therefore, sampling fluctuations are smaller in the quartz signals than in those from the scintillating fibers. Such fluctuations are thus not the factor limiting the em resolution of the quartz fiber readout. As was also found in previous tests of other quartz fiber calorimeters [3], the em resolution of the quartz component of our detector is completely dominated and determined by *photoelectron statistics*. On average, em showers produced 0.5 photoelectrons per GeV deposited energy in the quartz fibers. For 200 GeV em showers, the signal was thus, on average, composed of 100 photoelectrons. Statistical fluctuations in that number lead to an energy resolution of 10%.

The light yield was not the main limiting factor for the resolution measured with the scintillating fibers. Based on the light yield measured for similar calorimeters, we expect that the showers produced, on average, ~ 20 photoelectrons per GeV in our detector. At 200 GeV, the signals thus consisted of ~ 4000 photoelectrons and the statistical fluctuations in this number contributed about 1.6% to the energy resolution, which was measured to be 3.8% at this energy. In the scintillating fibers, the em energy resolution is dominated by sampling fluctuations. Such fluctuations are generally well described by the following formula [2]:

$$\frac{\sigma}{E} = 2.7\%\sqrt{d/f_{\text{samp}}}\frac{1}{\sqrt{E}} \quad (1)$$

in which the thickness d of the active layers is expressed in mm and f_{samp} is the sampling fraction for minimum ionizing particles. Since $d = 0.44$ mm and $f_{\text{samp}} = 2.8 \times 10^{-3}$, we expect sampling fluctuations to contribute $\sim 35\%/\sqrt{E}$ to the em energy resolution.

The electron measurements also illustrated very clearly the differences between the angular distributions of the scintillation light and the Cherenkov light produced by the shower particles. The scintillation light is emitted isotropically when excited molecules in the scintillating fibers return to their ground state. On the other hand, the Cherenkov light is emitted in a cone with a 46° opening angle centered around the direction of the relativistic shower particles. As the angle of the incident electron beam is changed, the quartz fibers pick up Cherenkov light emitted by shower particles that travel at a changing characteristic angle with the direction of the beam. In the standard configuration, with the beam entering perpendicular to the calorimeter's front face, both the x and y fibers are exclusively sensitive to Cherenkov light emitted by shower particles travelling at an angle of 44° (90° − 46°) with respect to the beam. However, as the angle of incidence is changed, the angle between the shower axis and the fibers oriented in one direction *decreases*, while the angle between the shower axis and the fibers oriented in the other direction *increases*. The larger the angle of rotation, the larger this effect becomes. It reaches a maximum when the angle of incidence is 90°. In that case, the fibers oriented in one direction make an angle of 45° with the shower axis and are thus exclusively sensitive to the most abundant shower particles, namely those travelling in the direction of the shower axis. The other fiber ribbons make an angle of 135° with the shower axis and thus produce a signal for relativistic shower particles travelling perpendicular to the shower axis.

In Fig. 6, the 200 GeV electron data are plotted as a function of the angle of incidence of the incoming particles. The figure shows that the ratio of the signals observed in the x and y scintillating fibers is essentially independent of this angle. On the other hand, the ratio of the signals observed in the x and y quartz fibers strongly depends on the direction of the showering particles, in the sense described above. Quantitatively, the observed effect is in good agreement with the angular dependence of the signals from em showers in a quartz fiber calorimeter reported by various authors [4,5].

The observed effect offers in principle the opportunity to use the dual-readout calorimeter as a *goniometer*. A comparison of the total signals

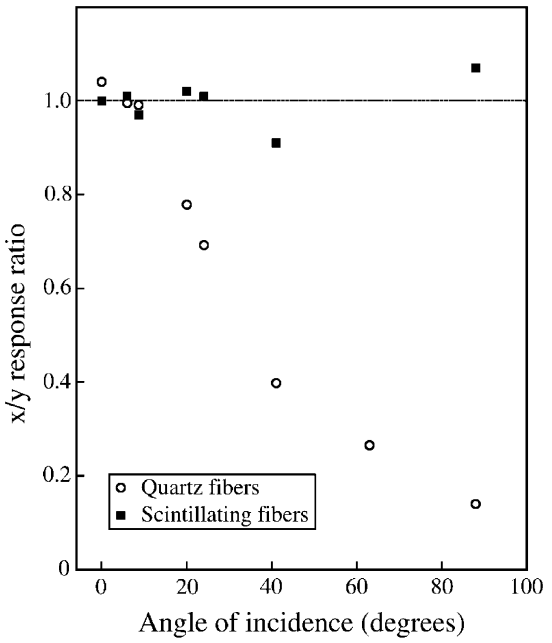

Fig. 6. Ratio of the signals measured in fibers oriented in the x and y directions, as a function of the angle of incidence of the showering electrons (200 GeV). Results are shown separately for the quartz fibers and for the scintillating fibers.

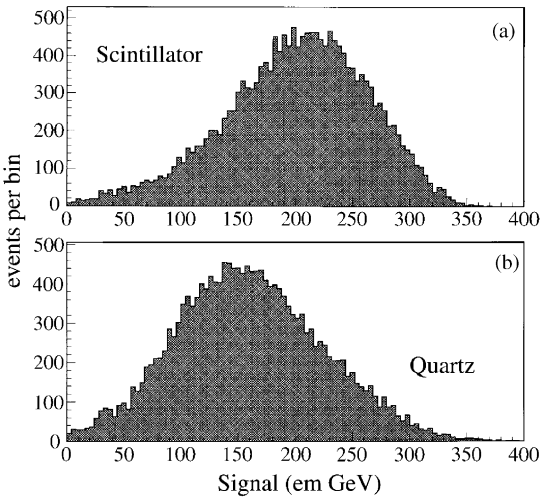

Fig. 7. Signal distributions for 375 GeV π^- detected in the dual-readout calorimeter. Shown are the signals from the scintillating fibers (a) and from the quartz fibers (b). The pions interacted in a $0.25\lambda_{\mathrm{int}}$ carbon target placed directly upstream of the calorimeter. See text for more details.

from the two perpendicular sets of quartz fibers provides information about the angle of incidence of the showering particles, a nice and unforeseen bonus.

3.2. Hadrons

3.2.1. Response function and energy resolution

Mainly as a result of the effects of incomplete shower containment, the signal distributions for high energy hadrons from this thin detector looked very different from the electron ones shown above.

Fig. 7 shows the signal distributions for 375 GeVπ^-, from the scintillating fibers (Fig. 7a) and from the quartz fibers (Fig. 7b). Only pions that started their shower in the second half of the upstream carbon target ($0.25\lambda_{\mathrm{int}}$) were selected for this figure. In this way, the leakage fluctuations were limited to those deriving from the shower development itself, disregarding the effects of fluctuations in the starting point of the showers. Separate studies showed that this event selection did not lead to biases in the topology of the event samples.

The horizontal scale of Fig. 7 is based on the calibration performed with electrons. The signals are thus on average, considerably smaller than those that would be produced by 375 GeV electrons. The quartz signals are, again on average, smaller than the scintillator signals. The difference is about 23%. Moreover, the shape of the quartz signal distribution is different from that measured with the scintillating fibers. The latter is skewed to the low-energy side, whereas the quartz signal distribution is skewed to the high-energy side. Apparently, the signals from both types of fibers do provide different information about the showering particles.

This becomes even more clear when we look at the signals event-by-event. In Fig. 8a, the 375 GeVπ^- signals recorded by the quartz fibers are plotted versus those in the scintillating fibers. There is clearly a non-linear correlation between these signals, which indicates that they indeed measure different characteristics of the showers.

The scintillator signal distribution, i.e., the projection of the scatterplot on the horizontal axis, is shown in Fig. 7a. The fact that this distribution is skewed to the low-energy side may be expected as a result of shower leakage. As we argued in Section 1, the relative strength of the quartz signal might be used as a handle on that leakage, event-by-event. Since the Cherenkov signal is predominantly produced by π^0 showers that are contained even in this thin detector, a relatively large (small) Cherenkov signal would indicate that a relatively small (large) fraction of the energy escaped from the detector. For this reason, we investigated the merits of the *ratio of the signals from the quartz fibers and from the scintillating fibers*, Q/S, as an event-by-event measure of the shower leakage.

In Fig. 8a, the signal ratio Q/S corresponds to the slope of a line through the bottom left corner of the scatter plot. The two lines drawn in this figure represent $Q/S = 1$ and $Q/S = 0.5$, respectively. Fig. 8b shows the distribution of the Q/S signal ratio. On average, this ratio amounted to 0.77 at 375 GeV. The average value of the Q/S distribution was not very different for the other energies at which we performed our studies. The fact that the Q/S ratio is smaller than 1.0 indicates that a significant fraction, typically 20–25%, of the scintillator signal in this detector is caused by *non-relativistic* shower particles, predominantly protons released from nuclei in spallation processes, or recoiling from elastic neutron scattering in the plastic fibers.

Fig. 9 shows the signal distributions measured with the scintillating fibers for 375 GeVπ^--induced showers, for subsets of events selected on the basis of their Q/S value. In Fig. 9a, the signal distribution is given for events with a small Q/S value ($Q/S < 0.45$). These events indeed populate the left-side tail of the calorimeter's response function (Fig. 7a). This distribution is very different from the one obtained for events with Q/S ratios near the most probable value, shown in Fig. 9b. The average values of the scintillator signal distributions in Figs. 9a and b differ by about a factor of two.

When selecting events with a large Q/S value, one would expect to be predominantly sensitive to showers in which a large fraction of the initial energy was used for π^0 production in the first interaction. Such events should be well contained in this detector and one would thus expect to select events from the high-energy tail of the spectrum. The signal distribution for events with a large Q/S value, shown in Fig. 9c, does indeed contain an anomalous fraction of events with a large pulse

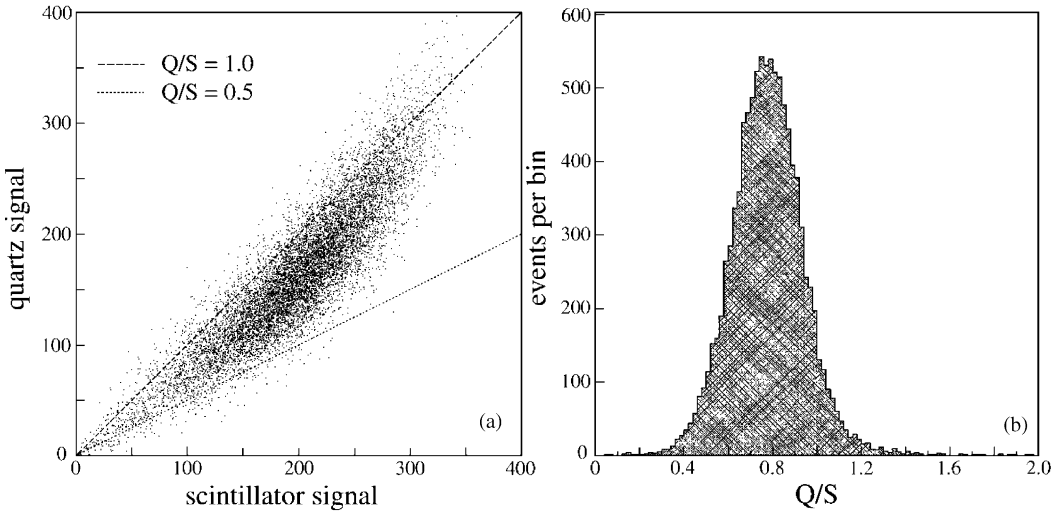

Fig. 8. Results of tests of the dual-readout calorimeter with 375 GeV pions. Scatter plot of the signals recorded in the quartz fibers vs. those in the scintillating fibers (a). Distribution of the ratio of the signals observed in the quartz fibers and the scintillating fibers (b).

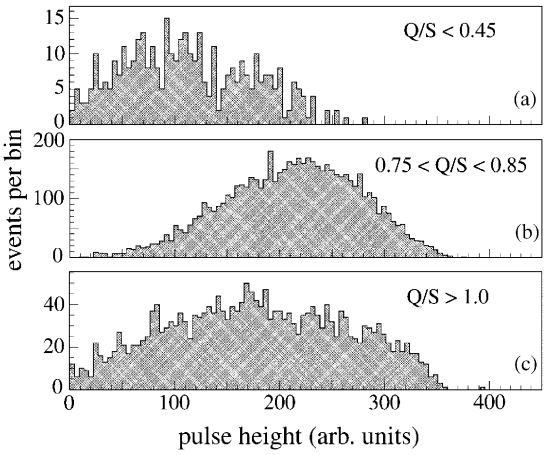

Fig. 9. Signal distributions in the scintillating fibers recorded for showers induced by 375 GeV π^-, for various subsets of events, selected on the basis of the value of their Q/S signal ratio.

height. However, it also contains an anomalous fraction of events with a small pulse height. This can be understood from the fact that at small pulse heights, the Q/S value is not well determined, mainly because of the small numbers of photoelectrons constituting the signals from the quartz fibers.

In any case, these results demonstrate that events from the tails of the Q/S distribution (Fig. 8b) correspond to events from the tails of the signal distribution measured with the scintillating fibers alone. We conclude from these results that the ratio of the signals from the quartz and the scintillating fibers does indeed provide information on the energy containment and thus could be used to reduce the fluctuations that dominate the response function of this very thin calorimeter.

We studied several methods of combining the signals from the quartz fibers and the scintillating fibers and investigated their effects on the response function. In the following, we describe one of these methods, which is particularly transparant and easy to apply.

The Q/S spectrum (see Fig. 8b) was divided into narrow bins, and for each bin the average scintillator signal was determined. This average was compared to the overall average scintillator signal and the ratio between these two averages was used as a correction factor. This correction factor turned out to be a smooth function of Q/S and was well described by a fourth-order polynomial function, $P_4(Q/S)$. The energy of showering particle i was then estimated as

$$E_i = \frac{aS_i}{P_4(Q/S)_i} \tag{2}$$

in which a is an overall normalization constant.

As described above, the tails of the S_i distribution are predominantly populated by events from the tails of the Q/S spectrum. It turned out that by eliminating events with anomalous Q/S values, a significant improvement in the energy resolution could be obtained. In addition, the resulting E_i distributions became considerably more symmetric than the raw S_i distributions.

Fig. 10 shows the improvement in the energy resolution for π^- showers at three different energies, as a function of the fraction of events that were eliminated from the distributions, based on their Q/S value. For example, by cutting 15% of the events from the tails of the Q/S distribution, the resolution improved by 8% at 150 GeV and by 12% at 375 GeV. The resolution improvement observed in the absence of event cuts (1–5% for

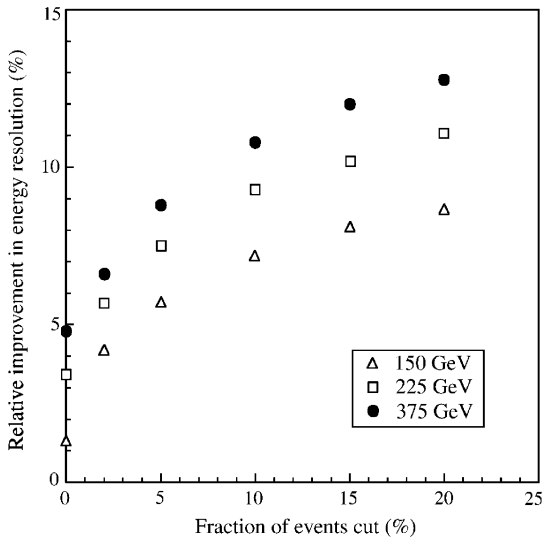

Fig. 10. Improvement in the energy resolution for 150, 225 and 375 GeV π^- as a function of the fraction of events cut from the tails of the Q/S distributions.

150–375 GeV) is the result of applying the correction factor (2).

The improvement in the response function that could be achieved with this and other methods turned out to be primarily limited by the light yield of the quartz fibers (0.5 photoelectrons/GeV, see Section 3.1). Fluctuations in the number of Cherenkov photoelectrons observed by the PMTs reading out the signals from the quartz fibers determined the width of the "banana" in Fig. 8a and thus the selectivity of Q/S cuts. This is the reason why the effects of the method (i.e., the improvement in the energy resolution) increase with increasing hadron energy (see Fig. 10).

Fig. 11 shows the fractional width of the distribution of the ratio of the signals from the quartz and the scintillating fibers (the "Q/S distribution"), as a function of the energy of the incoming pions. As before, this energy is plotted on a scale linear in $E^{-1/2}$, so that scaling with $[\sqrt{E}]^{-1}$ corresponds to a straight line through

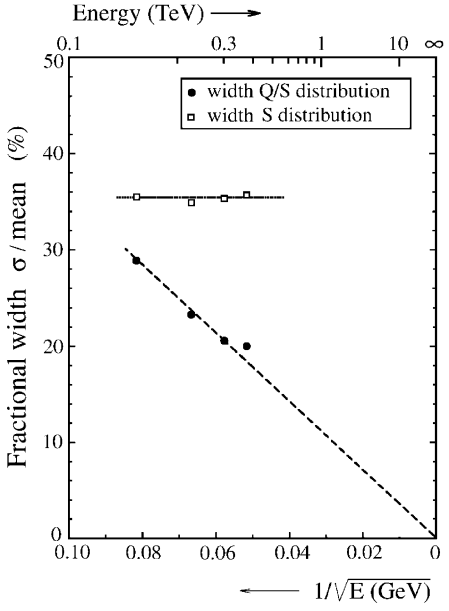

Fig. 11. The fractional width of the distributions of the signals from the scintillating fibers (S) and of the ratio of the signals from the quartz and the scintillating fibers for the same events (Q/S). The 150 GeV points were measured in the tertiary π^- beam, while secondary π^- beams were used to obtain the points at 225, 300 and 375 GeV.

the bottom right corner of this plot. The experimental data, which cover an energy range of 150–375 GeV, are well described by such a line. This means that the width of the Q/S distribution in this energy range is completely determined by fluctuations governed by Poisson statistics, i.e., fluctuations in the number of photoelectrons produced by Cherenkov light from the quartz fibers.

Not surprisingly, the width of the Q/S distribution turned out to be strongly correlated with the improvement in the energy resolution that could be obtained with methods such as the one described above. At 150 GeV, this method led to an improvement of 8%, whereas at 375 GeV, the resolution was improved by 12%.

As the energy is further increased beyond the limits achievable in our test-beam, towards the region of interest for the cosmic ray studies, a further improvement of the energy resolution may thus be expected from combining the data recorded by the two types of fibers in our calorimeter. This trend will continue, at least until the point where factors other than the light yield in the quartz fibers start dominating the width of the Q/S distribution. Since the width of the Q/S distribution continues to improve over the entire energy range accessible in these tests, the present data do not allow us to estimate the ultimate improvement in energy resolution that is achievable with our method.

However, we did find that the underlying relationship between the signals from the quartz fibers and the scintillating fibers did not change significantly over the energy range accessible to us in these studies. This is illustrated in Fig. 12a.

This relationship was determined by subdividing the $(Q+S)$ spectrum into narrow bins. For each bin, which is represented by a strip oriented perpendicular to the $Q/S=1$ line in Fig. 8a, we determined the average value of the signal from the scintillating fibers. These average values formed the "underlying banana curve" shown in Fig. 12a. The axes in this figure were scaled in such a way that the full scale corresponded to the electron signal for the chosen beam energy, both for the quartz fibers and the scintillating fibers. The figure shows the banana curves for 150, 250

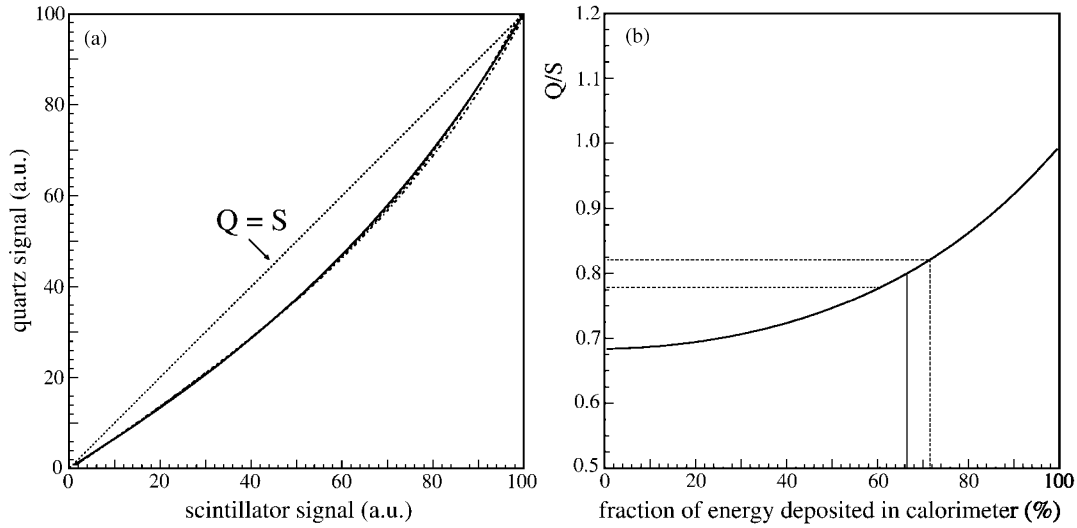

Fig. 12. The underlying relationship between the signals from the quartz fibers and the scintillating fibers. Fluctuations resulting from photoelectron statistics have been eliminated, and the scale is chosen such that the results are energy independent. Three "banana curves" for 150, 250 and 375 GeV are barely distinguishable (a). The relationship between the Q/S signal ratio and the energy fraction contained in the calorimeter (b). See text for details.

and 375 GeV, but these curves are so similar that they can be barely distinguished from each other.

A comparison of the Cherenkov and dE/dx signals from the same events provides complementary information about the showering particles, because these underlying banana curves differ significantly from the $Q = S$ line. This complementary information makes it possible to measure the energy of these particles more accurately than if only dE/dx information were available. Fluctuations about the underlying banana curve, resulting from the small yield of the quartz fibers, limited the improvement that could be achieved in our tests. However, even at this small light yield, the improvement could be very substantial at the high energies for which this detector is intended.

This is illustrated in Fig. 12b, where this measured "underlying banana" is translated into a relationship between the measurable quantity Q/S and the energy fraction deposited in the calorimeter. The Q/S values (i.e., the slopes of the points constituting the underlying banana curve) range from ~ 0.7 for events with a large leakage fraction to 1.0 for completely contained events. The precision with which the Q/S value can be measured experimentally will thus directly determine the precision with which the leakage fraction (and thus the shower energy) can be determined. Since a small change in the measured quantity (Q/S) may correspond to a much larger relative change in the fraction of contained energy, the contribution of fluctuations in the number of (Cherenkov) photoelectrons to the experimental precision of the hadronic energy measurement is larger than expected on the basis of Poisson statistics.

Let us consider, as an example, a showering hadron with an energy of 10 TeV. Let us, moreover, assume that this particle deposits a major fraction of its energy in our detector and that the resulting Q/S signal ratio is 0.80. In that case, the quartz signal would consist of ~ 2000–3000 photoelectrons, so that the experimental precision of the measured Q/S ratio would be about 0.02. Fig. 12b shows that this would allow us to conclude that this particle deposited between 60% and 72% of its energy in our detector. The energy of the showering particle could thus be found by multiplying the recorded scintillator signal by $(0.66 \pm 0.06)^{-1}$.

Fig. 12b shows that the sensitivity and reliability of this method increases as a larger fraction of the shower energy is deposited in the calorimeter. This is no surprise. If an incoming hadron interacts in the calorimeter and produces few or no energetic π^0s, the resulting signals are not very dependent on the energy of the incoming particle, since most of the reaction products escape from the detector. It is, in that case, not well possible to make an accurate estimate of the energy of the incoming particle. One could, for example, find on the basis of the Q/S ratio that $90 \pm 10\%$ of the shower energy escaped detection. However, that would only set a lower limit to the energy of the showering particle.

3.2.2. Hadronic signal linearity

So far, we have concentrated on the energy resolution and the shape of the hadronic response function. In this subsection, we want to address briefly another parameter that is of great importance for the calorimeter performance: The hadronic response, i.e., the average signal per unit of energy.

It is a well known fact that most hadron calorimeters are non-linear, as a consequence of non-compensation ($e/h \neq 1$). If $e/h > 1$, which is typically the case, the hadronic response increases with energy, since the average shower fraction carried by the em shower component increases with energy [2].

The calorimeter described in this paper clearly deviates from this rule. This is illustrated in Fig. 13, which shows the hadronic response, derived from the uncorrected scintillating fiber signals, as a function of the pion energy. Over the energy range for which the measurements were carried out, the response was constant within the experimental uncertainties, with possible non-linearities below the 1% level.

This characteristic is a consequence of the fact that the calorimeter is very thin. The increasing em shower fraction mentioned above is a consequence of the fact that, on average, the number of generations in the shower development increases with energy and in each generation some fraction of the energy carried by the remaining shower particles is used to produce π^0s [2]. However, our calorimeter only detects the early phase of the shower development, i.e., the first few generations of shower particles, *independent of energy*. As a result, the hadronic response is independent of energy as well.

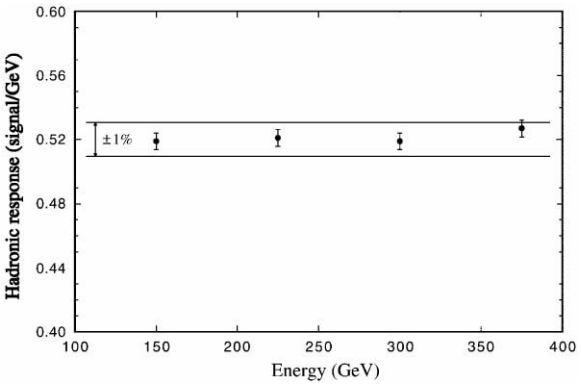

Fig. 13. The hadronic response (average signal per unit energy) of the calorimeter, derived from the uncorrected scintillator signals, as a function of energy. The vertical scale is normalized to that for electrons, measured with the same device.

4. Summary and conclusions

We have tested a hadron calorimeter that is based on the novel concept of measuring the properties of the developing showers with two different active media that provide complementary information about the particles that initiated the showers. By measuring both the scintillation light and the Cherenkov light generated in hadron-induced showers, the energy containment in this very thin detector ($1.4\lambda_{\text{int}}$) could be estimated event-by-event. Since fluctuations in the energy containment dominate the performance of this device, this information made it possible to improve the response function, both in terms of energy resolution and in terms of shape, by eliminating non-Gaussian tails.

A crucial parameter in this context turned out to be the ratio of the signals from the quartz fibers and the scintillating fibers, Q/S. Events in which a large fraction of the energy of the incoming particle was spent on π^0 production, and which were thus well contained in the calorimeter, were

characterized by a large Q/S value, whereas a small Q/S ratio was indicative for relatively little em shower activity, and thus relatively large shower leakage.

We have shown that the beneficial effects of our method were limited by the small light yield of the quartz fibers, only 0.5 photoelectrons per GeV. We have also shown that the underlying relationship between the signals from both types of fibers, which is responsible for the beneficial effects of our method, is independent of energy, at least in the energy range accessible in our test beam experiments. Should this trend continue at higher energies, very substantial benefits of our method may be expected in the multi-TeV energy range for which this device is intended. We have shown that, for example, at 10 TeV energy resolutions of the order of 10% may be expected in that case.

Since higher-energy particle beams are not readily available at the present time, the only alternative method to explore the limits of the improvement achievable with our method and thus test the validity of the above prediction consists of increasing the light yield of the Cherenkov channels of our detector. This can be done by adding more quartz fibers, by increasing the numerical aperture of the fibers, by increasing the quantum efficiency of the light detectors, or by some combination of these methods. We are planning to repeat the described tests in the near future with a significantly improved Cherenkov light yield.

The development of the dual-readout calorimeter described in this paper was inspired by the needs of high-energy cosmic ray experiments outside the Earth's atmosphere. Detector mass comes at a very high cost in these experiments and, therefore, methods that maximize the experimental information per unit detector mass are of crucial importance. However, it is likely that the dual-readout technique discussed here has also interesting applications in detectors where mass limitations do not play a role and where shower containment is thus not a critical issue. For example, fluctuations in the em content of high-energy hadron showers could be measured with excellent precision in a relatively small detector volume, i.e., that needed for the containment of the em shower core. This would make high-resolution hadron calorimetry possible, without the need to integrate the signals over a multi-ton detector volume, as in compensating calorimeters based on the contribution of neutrons to the detector signals [6].

Coming back to the needs of limited-mass cosmic ray experiments outside the Earth's atmosphere, we would like to point again to Fig. 11. This figure also shows the energy dependence of the hadronic energy resolution measured with the scintillating fibers *alone*. This resolution is essentially independent of energy, which illustrates the fact that the light yield of the scintillating fibers is by no means a determining or limiting factor for this resolution. Since the hadronic resolution is completely dominated by fluctuations in shower leakage, a sampling calorimeter with a sampling fraction of less than 0.3% such as this one is thus as good (or bad) for hadron detection as a detector consisting of homogeneously sensitive scintillator material (e.g., bismuth germanium oxide) with the same depth. Only by addressing the fluctuations that dominate the resolution, i.e., the fluctuations in shower containment, can one hope to improve this performance, as illustrated by the results presented in this paper.

Acknowledgements

We would like to thank our colleagues from NASA and CERN, in particular John Mitchell, Paul Hink and Mark Christl, for their interest and assistance in the various tests described in this paper. We are grateful to Niels Doble, who provided us with particle beams of excellent quality, and to Dragoslav Lazic, who helped us with the data acquisition system. This project was carried out with financial support from NASA, under grant number NRA-97-OSS-13.

References

[1] N. Akchurin et al., Nucl. Instr. and Meth. A 399 (1997) 202.

[2] R. Wigmans, in: Calorimetry—Energy Measurement in Particle Physics, International Series on Monographs in Physics, Vol. 107, Oxford University Press, Oxford, 2000.
[3] N. Akchurin et al., Nucl. Instr. and Meth. A 408 (1998) 380.
[4] G. Anzivino et al., Nucl. Instr. and Meth. A 360 (1995) 237.
[5] O. Ganel, R. Wigmans, Nucl. Instr. and Meth. A 365 (1995) 104.
[6] R. Wigmans, Quartz fibers and the prospects for hadron calorimetry at the 1% resolution level, Proceedings of the Seventh International Conference on Calorimetry in High Energy Physics, Tucson, 1997, World Scientific, Singapore, 1998, p. 182.